Energy Conversion and Management: X 27 (2025) 101135

Contents lists available at ScienceDirect

Energy Conversion and Management: X

journal homepage: www.sciencedirect.com/journal/energy-conversion-and-management-x

# Boosting sustainable hydrogen production through the gasification of biorefinery sludges[☆]

Martin J. Taylor [a,*], Karl Hornsby [a], Kin Wai Cheah [b], Adrian Chun Minh Loy [c], Peter Hurst [d], Mark Gronnow [d], Katie Chong [e], Patrick Kelly [f], Simon Walker [f], Vasiliki Skoulou [a]

[a] *School of Engineering and Technology, Chemical Engineering, University of Hull, Cottingham Road, Hull HU6 7RX, United Kingdom*
[b] *School of Computing, Engineering and Digital Technologies, Teesside University, Borough Road, Middlesbrough TS1 3BA, United Kingdom*
[c] *Department of Chemical Engineering, The University of Melbourne, Victoria 3010, Australia*
[d] *Biorenewables Development Centre, Unit 1 Hassacarr Ln, Chessingham Park, York YO19 5SN, United Kingdom*
[e] *Energy and Bioproducts Research Institute, Aston University, Aston Triangle, Birmingham B4 7ET, United Kingdom*
[f] *Jesmond Engineering Ltd, Baffin Way, Brough HU15 1YU, United Kingdom*

ARTICLE INFO

*Keywords:*
Hydrogen
Gasification
Bio-refinery waste
Hydrolysis
Waste management

ABSTRACT

Decarbonisation of energy production is vital to prevent further climatological disasters; sustainable hydrogen production from unique underutilised feedstocks will presents a viable pathway to overcome further energy crises and transition away from fossil reserves. By tapping into severely underutilised lignin-rich biorefinery waste streams such as sludges, produced post hydrolysis (sugar extraction, pre-fermentation), a wealth of hydrogen was unlocked via gasification at 950 °C in 1 % $O_2/N_2$, producing a gas-rich product mixture (>70 wt%) in a batch downdraft reactor. Subject to an optimised pre/post-treatment regime, low nitrogen and ash (<2 wt%) containing 1–2 mm sludges derived from barley and wheat straws were found to create a producer gas with hydrogen concentrations of 27.95 vol.% and 22.12 vol.%, respectively, as a result this work has pioneered a waste-to-hydrogen pathway for biorefinery sludges, achieving competitive $H_2$ yields without energy-intensive steam/catalysts. The formed sludges were found to be superior to both raw and leached parent feedstocks without NaOH hydrolysis, in terms of hydrogen production and solid fuel calorific values.

## 1. Introduction

Energy security is constantly shifting, this leads to periods of abundancy and sustainable development, it also leads to energy poverty and the switching back to fossil reserves so that demand can be met. To ensure that energy insecurity doesn't lead to a reverse transition, back towards traditional energy production and the consumption of fossil fuel. Global efforts are required to continue decarbonisation efforts by seeking renewable energy, especially through bio-renewables. One such option are lignocellulosic waste streams, such materials can be the produced from food processing industries, agricultural waste streams and emerging biorefinery wastes, otherwise known as second generation resources [1–3]. A second-generation feedstock is one that doesn't compete with food production, therefore aligning with the United Nations Sustainable Development Goal of Zero Hunger, while supporting Affordable and Clean Energy, as well as Responsible Consumption and Production, along with Climate action. For the latter goal, lignocellulosic biomass wastes are considered as a short-term substitution of traditional fossil-based solid fuels, together with other forms of renewable energy, collectively true net carbon reductions ($CO_2$) can take place. However, much like fossil residues before them, a possible solid fuel cannot be effectively used directly from the land, the fuel candidate must be pre-treated to ensure long term energy production.

Waste pre-treatment options range from overall material size, removal of surface bound or soluble impurities and moisture, or approaches where a material can be modified to enable greater reactivity by expanding the available surface area for biochemical or thermochemical conversion [4]. However, alike with many well-established solid fuels, thermochemical conversion routes for energy production, be that combustion or gasification all lead to the same problem, reactions between carbon rich materials in oxygen, in any concentration will liberate $CO_2$ through a combustion pathway. Therefore, alternative

---

[☆] This article is part of a special issue entitled: 'Biofuels' published in Energy Conversion and Management: X.

[*] Corresponding author.
*E-mail address:* Martin.Taylor@hull.ac.uk (M.J. Taylor).

https://doi.org/10.1016/j.ecmx.2025.101135
Received 27 March 2025; Received in revised form 1 July 2025; Accepted 2 July 2025

fuel production routes to overcome this problem, or methods of changing reaction selectively to promote the production of hydrogen ($H_2$) from waste sources are vital for us to decarbonise energy production from solid fuels. Hydrogen is the apex of low carbon fuels and has an energy density of ~ 60 % higher than natural gas or bio-methane [5]. Therefore, by combining waste to energy with appropriate carbon removal technologies, will enable $CO_x$ lean gaseous fuel production. Carbon dioxide can be removed from the produced gas feed post-combustion/gasification of fuel, pushing energy production into the realms of negative emissions.

Although for complete decarbonisation, not just the energy production sector by the 2050 goal, it is projected that the required $H_2$ production must rise to 512 Mt between 2030 and 2050 [6,7]. To reach this level of production, there is no one-size fits all approach, sustainable hydrogen production must be approached in a dual symbiotic way, much like sustainable energy on a whole, albeit for the case of $H_2$ it is currently stifled by current technology readiness. There are vast global investments into electrolysers that are steadily becoming more efficient, although their lifetimes are still not on par with more established technologies [8,9]. Electrolysis is a process where water is separated into $H_2$ and $O_2$, a rapid approach to hydrogen production but seriously hampered by cost due to high electrical demand [10]. Another approach is the decomposition of ammonia ($NH_4$), a compressible liquid hydrogen carrier which allows for the zero-carbon liberation of hydrogen via a thermal cracking route or electrocatalytic pathway [11]. However, $NH_4$ is an invaluable chemical for fertilisers, production/manufacturing, refrigeration, water purification and pharmaceuticals, by considering how versatile $NH_4$ is, its role as a bulk energy source could be considered minor unless production is rapidly increased, much like hydrogen. This does leave behind technologies such as methane reforming which is carried out using heterogeneous catalysis and other emerging technologies such as plasma-assisted pyrolysis [12]. These methods often use natural gas, although not exclusive, and generate an amorphous carbon secondary product, carbon black [12]. While considered a cost-effective method of producing hydrogen, the high carbon footprint of natural gas, especially through extraction is a carbon intensive practice ($11 - 21$ g $CO_2e\ MJ^{-1}_{LHV}$) [13]. The more sustainable pathway for $H_2$ is through the transformation of lignocellulosic wastes as an option for sustainable hydrogen production via gasification [14].

Gasification utilises a critically dilute oxygen atmosphere (1–5 vol. %) which does not fully oxidise the carbon in the way that combustion will ($CO > CO_2$) [15]. By doing so, the produced gas mixture from gasification is denoted as syngas (synthesis gas) which generally contains CO, $CO_2$, $CH_4$, $H_2$ and trace short chain hydrocarbons ($C_xH_y$). By augmenting gasification with steam, catalysis or a combination of both will drive various reactions to boost hydrogen yields, these include the water–gas shift (WGS) reaction (Eq. (1), WGS (Eq. (2), steam reforming of tar (Eq. (3) and steam reforming of methane (Eq. (4) [16–19].

$$CO + H_2O \leftrightharpoons CO_2 + H_2\ (-41\,\mathrm{kJ\,mol} - 1) \quad (1)$$

$$C + H_2O \leftrightharpoons CO + H_2\ (+130\,\mathrm{kJ\,mol} - 1) \quad (2)$$

$$\mathrm{Tar} \rightarrow CO_x + C_xH_y + H_2\ (\mathrm{Variable}) \quad (3)$$

$$CH_4 + H_2O \leftrightharpoons CO + 3H_2\ (+206\,\mathrm{kJ\,mol} - 1) \quad (4)$$

The push for utilising lignocellulosic biomass feedstocks is rooted through the sheer number of available options and for some feedstocks, substantial abundancy. However, positives can be masked in a disadvantage, each feedstock has a unique organic and inorganic composition [20]. The extractable organic components, namely cellulose and hemicellulose hold greater value than simply converting for energy production. These are high-value sugars, hexose and pentose, that can be fermented (value added) into various fine chemicals and liquid fuels, stimulating the green and sustainable chemical economy. Post sugar extraction, the final organic residue lignin remains, which can be difficult to isolate and effectively utilise without high energy and or prolonged processing. As a result, lignin, the rugged polymer backbone of lignocellulosic biomass is often committed to waste and or classified as a low-value material, used previous use in animal feeds or as a component in adhesives [21,22]. Lignin and specifically, lignin-derived wastes hold a far greater stake in both the bioeconomy [23] and broader circular economy [24] that could display its true value in use in the emerging hydrogen economy [25]. Lignin utilisation stands out as a sustainable option to producing hydrogen that is not dependant on electrolysis, methane pyrolysis or the use of solid fossil fuels [26]. To enable this proposal, lignin-rich biorefinery waste streams (high moisture species post sugar hydrolysis) must be post-processed to increase their value by decreasing their overall ash content, often inflated by the impregnation of alkali or alkaline earth metals, sulphur or chlorine [4,27–30]. It is well known that at scale, ash deposits lead to systematic disruptions along the waste to energy process, such as reactor defluidisation (subject to reactor configuration), heat exchanger fowling and reactor hot spots [31]. Additionally, ash residues can facilitate rogue reactions or downstream product instability [32–35]. The former is driven by the fact that ash can act catalytically for the various gasification reactions, especially Na and K for the WGS reaction (Eq. (1), as discussed in previous works [14,16]. Therefore, to ensure that an operator has full control over the gasification, the process must accommodate means to drive down ash concentration and remove such elements to prevent undesired reactions, albeit stifling ones of benefit [36].

This work builds upon the Bluegen Project, DESNZ Hydrogen BECCS Innovation Programme: Phase 1 [7]. Here, the effect of varying NaOH concentrations (0.2 M, 0.4 M and 1.0 M) on two globally abundant lignocellulosic biomass waste streams, barley straw and wheat straw for producing hydrogen from lignin rich sludges is discussed. Specifically, investigating whether there is a correlation between increasing the base concentration, and base pre-treatment residence time on the effect of hydrolysis (removal of high-value cellulose and hemicellulose sugar units) on subsequent hydrogen yields in producer gas during gasification without catalysis and or steam addition, under batch conditions. Unlike many prior studies focused on catalytic gasification of raw biomass materials [37–41], this work is the first to demonstrate the valorisation of post-hydrolysis biorefinery sludges (high-moisture, lignin-rich waste) for $H_2$ production via gasification without steam/catalysts. The novelty of this work aims to address the sludge-specific pre-treatment and transform underutilized sludge into a high-potential $H_2$ feedstock, as emphasized in the Bluegen Project report. This work pioneers a waste-to-hydrogen pathway for biorefinery sludges, achieving competitive $H_2$ yields without energy-intensive steam/catalysts.

## 2. Experimental Section

### 2.1. Feedstock preparation

Barley straw and wheat straw, grown locally, was milled using a Retsch SM300 cutting mill fitted with a 1.00 mm screen. The milled grains were treated with varying concentrations of NaOH (0.2 M, 0.4 M and 1.0 M, Fisher Scientific) across two residence times under batch conditions for 0.5 h and 1.0 h at 90 °C in a 10 L Universal Process Machine (RoboQbo 15–4). This was followed by drying at 105 °C in a Genlab OV/100/F/DTG oven overnight. The resulting cake was hammer milled using a Retsch GM200 Grindomix Knife Mill at 4000 rpm for 1 min (blunt edge of the blade for low sheer, separating the cake instead of reducing the grain size further). The resulting material was separated using a Retsch AS200 Vibratory Sieve Shaker, reclaiming the 1.00–2.00 mm fractions to ensure continuity. Each reclaimed feedstock was water washed (leached) in deionized water using a Heidolph Hei-Tec hotplate at 25 °C, 900 rpm for 24 h at a ratio of 10 g $L^{-1}$. The temperature was monitored using a Pt1000 thermocouple based in the leachate. The leached feedstocks were decanted and separated from their leachates, drying under *vacuo*, followed by thermally drying in a Fisherbrand gravity convection oven for 24 h at 105 °C.

### 2.2. Feedstock characterisation

Thermal degradation of the sludge derived materials was carried out using a LECO 701 thermogravimetric analyser (proximate analysis) where moisture, devolatilization, ash, higher heating value (HHV, gross calorific value) and lower heating value (LHV, net calorific value) were measured and calculated using the HHV and LHV equations shown in Table 1. The method carried out for analysis is detailed in earlier works [30,42]. Ultimate analysis (carbon, nitrogen and hydrogen) of all feedstocks was acquired using a LECO 628 CHN Combustion analyser using sample sizes of 50.00–60.00 mg. Fourier Transform Infrared spectra were obtained using a Thermo Scientific Nicolet iS5 with a PIKE MIRacle single reflection horizontal ATR accessory. Scanning Electron Microscopy (SEM) images were acquired via a Zeiss EVO 60 instrument at $10^{-2}$ Pa and an electron acceleration voltage of 20 kV. Powders were adhered to a coated conductive carbon tape and attached to the specimen holder. Bomb calorimetry was carried out on sample sizes between 0.80 and 1.00 g using a Parr 6200 Isoperibol calorimeter fitted with a Parr 1108P oxygen combustion vessel with an $O_2$ pressure of 450 psi. Leachate-based Na cations were quantified by a Dionex ICS 2000 system using a Dionex IonPac AS16 (2 x 250 mm) column, calibrating with a five-point calibration plot between 12.5 ppm and 200 ppm.

Hemicellulose and cellulose removal was characterised by using a modified Van Soest method dictated by Liang [43]. Once the feedstocks were initially treated and washed, the dried residues were added to 70 mL HCl (2 M) (Fisher Scientific), heating at 100 °C for 50 min, followed by washing until the washings ran to pH 7. The materials were then washed with 100 mL ethanol and acetone (Fisher Scientific, Analytical reagent grade, >99.8 %) before drying overnight, the change in mass from the HCl processing can be attributed to the digestion of hemicellulose. Cellulose was digested by adding 10 mL $H_2SO_4$ (Fisher Scientific, ACS, 95.0–98.0 %) to the dried material immediately transferred from the oven. The acid suspension aged for 4 h at 20 °C in a static environment before diluting in 90 mL deionised water further aged overnight at room temperature. The feedstock was dried, and the resulting mass loss was ascribed to be the loss of cellulose. The full change of mass was then compared with virgin feedstocks and the percentage reduction in hemicellulose and cellulose is shown in **Table S1**.

### 2.3. Gasification of sludge feedstocks

The gasification of the leached sludge feedstock was carried out in a lab scale, downdraft fixed-bed stainless steel, batch atmospheric reactor under a controlled reactive atmosphere. Here, dry synthetic air ($O_2$ 20 vol.% and $N_2$ 80 vol.%) was diluted by a mass flow controller (Aalborg, GFCS-01) with nitrogen to achieve a 1 % $O_2$ in $N_2$ mixture at a flow rate of 40 mL $min^{-1}$, corresponding to ~0.2 s of gas residence time. The gasifier was heated to 950 °C, measured by a K-type thermocouple positioned in the sample holder of the reactor. The heating rate was calculated to be ~50 ∘C $min^{-1}$, by measuring the time to reach $T_{max}$ from room temperature, holding for an additional 5 min at maximum temperature for a total reaction time of 23.5 min. Gas products were purified by a liquid tar trap (deionised water) and dried ($SiO_2$ gel, 70–230 mesh, Alfa Aesar) before storing in a 1 L Tedler bag and analysing offline using a Pollutek Gas 3000P analyser, gasification heats were ran in triplicate and the volumetric data was averaged, statistical variation in measurements is attributed to sample homogeneity (particle size and ash rich/deficient regions) and mass of feedstock charge used. The final product composition data was normalised by removing nitrogen from the mixture. Post reaction, the reactor was cooled to room temperature and cleaned in acetone to recover both the solid and liquid products from the reactor body and tubing. Once filtered from the char the tar/oil residues were separated via rotary evaporation and weighed to determine the individual product distributions. Between reaction sets, the reactors were cleaned in flowing air (40 mL $min^{-1}$) to combust organic residues and prevent follow on contamination.

**Table 1**

Proximate and ultimate analysis of leached barley and wheat straw derived sludges, at different NaOH concentrations and two residence times [7].

| Feedstock | | Hydrolysis time (min) | Moisture (wt.%) | Volatile (wt.%) | Fixed Carbon (wt.%) | Ash (wt.%) | HHV (MJ $kg^{-1}$) | LHV (MJ $kg^{-1}$) | C (wt.%) | H (wt.%) | N (wt.%) | O (wt.%)* | C/H ratio | C/N ratio | Calorific value (kJ $kg^{-1}$) |
|---|---|---|---|---|---|---|---|---|---|---|---|---|---|---|---|
| **Barley Straw** | 0.2 M | 30 | 2.82 | 86.06 | 9.67 | 1.45 | 16.82 | 14.44 | 43.00 | 6.11 | 0.19 | 49.25 | 7.04 | 224.08 | 18.55 |
| | 0.2 M | 60 | 1.36 | 83.99 | 9.96 | 4.70 | 16.58 | 14.48 | 45.30 | 6.71 | 0.03 | 43.26 | 6.75 | 1680.89 | 17.80 |
| | 0.4 M | 30 | 3.76 | 83.76 | 9.65 | 2.93 | 16.45 | 13.73 | 45.40 | 6.81 | 0.17 | 44.69 | 6.67 | 259.81 | 17.45 |
| | 0.4 M | 60 | 1.51 | 87.78 | 5.50 | 5.21 | 15.59 | 13.43 | 44.80 | 6.80 | 0.11 | 43.08 | 6.59 | 390.11 | 17.33 |
| | 1.0 M | 30 | 1.96 | 84.50 | 10.94 | 2.59 | 17.02 | 14.75 | 44.60 | 6.72 | N/D | 46.24 | 6.64 | – | 16.98 |
| | 1.0 M | 60 | 4.36 | 82.93 | 9.96 | 2.75 | 16.43 | 13.58 | 43.10 | 6.63 | 0.01 | 47.51 | 6.50 | 3243.04 | 17.17 |
| **Wheat Straw** | 0.2 M | 30 | 2.11 | 85.72 | 10.44 | 1.73 | 17.04 | 14.78 | 46.20 | 6.51 | N/D | 45.56 | 7.10 | – | 19.01 |
| | 0.2 M | 60 | 6.53 | 81.46 | 10.33 | 1.68 | 16.34 | 12.99 | 44.20 | 6.48 | 0.03 | 47.61 | 6.82 | 1308.47 | 17.01 |
| | 0.4 M | 30 | 2.81 | 84.69 | 10.98 | 1.52 | 17.07 | 14.60 | 44.20 | 6.59 | 0.11 | 47.58 | 6.71 | 391.22 | 15.34 |
| | 0.4 M | 60 | 2.52 | 85.31 | 10.74 | 1.44 | 17.09 | 14.65 | 46.50 | 6.89 | N/D | 45.29 | 6.75 | – | 18.08 |
| | 1.0 M | 30 | 2.98 | 86.26 | 9.39 | 1.44 | 16.76 | 14.19 | 45.80 | 6.94 | N/D | 45.85 | 6.60 | – | 17.32 |
| | 1.0 M | 60 | 1.51 | 86.74 | 10.24 | 1.51 | 17.13 | 14.98 | 44.20 | 6.61 | N/D | 47.86 | 6.69 | – | 17.25 |

HHV – Higher Heating Value, HHV = (0.3536 (FC)) + (0.1559(VM)) – (0.0078(ASH)).

LHV – Lower Heating Value (LHV) = HHV – (0.212 (Hydrogen content)) – (0.0245 (Moisture)) – (0.008 (Oxygen content)).

N/D – Not detectable.

*O (wt.%) is calculated by the following equation O = 100 − [ash (wt.%) + C (wt.%) + N (wt.%) + H (wt.%)].

## 3. Results and Discussion

### 3.1. Feedstock characterisation

As mentioned, the reclaimed sludges were leached (water washed) to extract the impregnated $Na^+$ ions from the hydrolysis pre-treatment, as well as other water-soluble ash constituents. Leaching was carried out over a 24 h period to maximise the inorganic removal from each feedstock. It was shown in our earlier work that some elements benefit from prolonged residence times to increase removal [33]. However, for Na due to its high solubility in water, it was found that was no further removed after 4 h. This was confirmed by ion chromatography where aliquots of the leachate were removed and filtered (0.25 µm Whatman syringe filter) across three particle size ranges to investigate the effect of feedstock physical surface area and Na diffusion. The data shows that the target feedstock size of this work (1–2 mm) inherently contained less $Na^+$ than other smaller particle sizes, albeit all three reached maximum removal at the same time point, an exemplar of this is shown in **Fig. S1** for barley straw, 0.2 M (60 min). The overall properties of each feedstock are reported in Table 1 which clearly shows that the ash content can be lowered to a point that can be considered a baseline for all feedstocks, where a 1.0 M NaOH hydrolysis reaction does not generate a feedstock with an inflated inorganic content, post leaching. Table 1 does show that the effect of base concentration has a mildly positive effect on the overall hydrogen content of the wheat straw derived feedstocks, whereas the opposite trend is seen for the barley straw derived sludges, indicating a contrasting effect on the hydrolysis process. Across the range of feedstocks there is an overall decrease in the C:H ratio for both families of sludges, as the concentration of NaOH used increases, this is due to two carbon components of the lignocellulosic matrix being removed, cellulose and hemicellulose, validated by **Table S1** which shows a gradual reduction in both sugar species as NaOH concentration and time increased. On the back of this, there is also a slightly lower calorific value along the series of samples, where barley straw sludge decreased from 18.55 kJ $kg^{-1}$ to 16.98 kJ $kg^{-1}$ moving from 0.2 M−1.0 M NaOH, respectively. A lower calorific value was also seen for wheat straw derived sludges, decreasing from 19.01 kJ $kg^{-1}$ to 17.25 kJ $kg^{-1}$ from 0.2 M−1.0 M NaOH, respectively, directly related to a decrease in C as the base concentration used was increased. Interestingly, by increasing the concentration of base used before leaching, there has been a complete removal of nitrogen in the feedstocks (Table 1). This is beneficial as there will be less $NO_x$-derived molecules formed during thermochemical conversion that is directly related to the feedstock.

Further chemical characterisation was carried out using Fourier Transform Infrared Spectroscopy (FTIR), this data is presented in Fig. 1**a** (barley straw) and Fig. 1**b** (wheat straw). By directly comparing each sludge-based feedstock with the parent waste feedstock, leached but not pre-treated with base, one can see there has been a substantial alteration to much of the chemical structure. Attention can be drawn to peaks such as 890 $cm^{-1}$ (glycosdic linkages of xylan) which is present in both Fig. 1**a** and Fig. 1**b** and decreases in intensity for wheat straw (Fig. 1**b**) but is not present for barley straw sludge 1 M at 60 min (Fig. 1**a**) [44]. There has been a substantial decrease in intensity at 1037 $cm^{-1}$, representing C-O, C=C and C-C-O stretching for woody aspects of the waste [30,33,44]. Next a cellulose/hemicellulose stretch at 1160 $cm^{-1}$, showing C-O-C asymmetric stretching has lost intensity from 0.2 M NaOH at 30 min [45]. Interestingly, there has been a number of peak at 1243 $cm^{-1}$, 1370 $cm^{-1}$, 1425 $cm^{-1}$ and 1596 $cm^{-1}$ which are evidence of conjugated ketones, C-H bending, C-H plane deformation and aromatic C=C stretches or C=O stretching, respectively [46]. All four of these mentioned sections are usually observed for lignin, however, it is logical to believe that some of this bonding and or structure can be altered as the polymeric matrix changes when hexose (cellulose derived sugar units) and pentose (hemicellulose derived sugar units) molecules are removed. This may influence the loss of intermolecular interactions (shown previously after leaching in water), as well as minor disturbances in bonding between lignin and cellulose/hemicellulose [33].

As well as these losses, there is an element of surface adsorbed $CO_2$ detected, highlighted by a red box, this is a feature caused during data acquisition. Finally, across the board, there is also the characteristic stretch at 3400 $cm^{-1}$ representing moisture, which is common due to the hygroscopic nature of lignocellulosic biomass, it could also be assigned to the alcohol component of lignin (–OH) [47].

Fig. 2 presents representative scanning electron microscope (SEM) images for the leached feedstocks **(**Fig. 2**a, 2b, 2d and 2e**) and produced sludges including 0.2 M 30 min barley straw derived sludge (Fig. 2**c**), and 0.2 M 30 min wheat straw derived sludge (Fig. 2**f**). The sludge feedstock images show a radically altered surface structure, even when using a low concentration of base, compared with images of the parent feedstock along their top topography (Fig. 2**a** and Fig. 2**d**), as well as at the cut edge which shows the internal channels (Fig. 2**b** and Fig. 2**e**). The relatively low magnification images clearly show that both feedstocks have lost their ordered and regular structure, in place the 0.2 M NaOH has generated a warped and irregular structure, especially at the ends of the grains which appear to have lost their channel structure post depolymerization though base hydrolysis.

Thermogravimetric analysis of the two sludge feedstock families (Fig. 3**a**-Fig. 3**d**), except for slightly different moisture contents (Table 1) follow the exact same weight loss profiles between one and other, these are shown in Fig. 3**a** for barley straw derived sludges and Fig. 3**c** for wheat straw derived sludges. These feedstock similarities are also extended to the DTG curves where the first derivative weight loss data

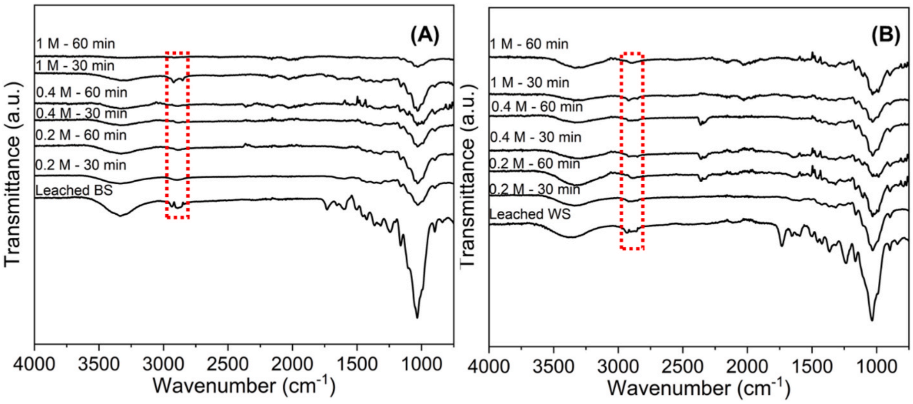

**Fig. 1.** Stacked FTIR spectra of (A) Leached barley straw (BS) and barley straw derived sludges, (B) Leached wheat straw (WS) and wheat straw derived sludges. The red box indicates atmospheric adsorbed $CO_2$. (For interpretation of the references to colour in this figure legend, the reader is referred to the web version of this article.)

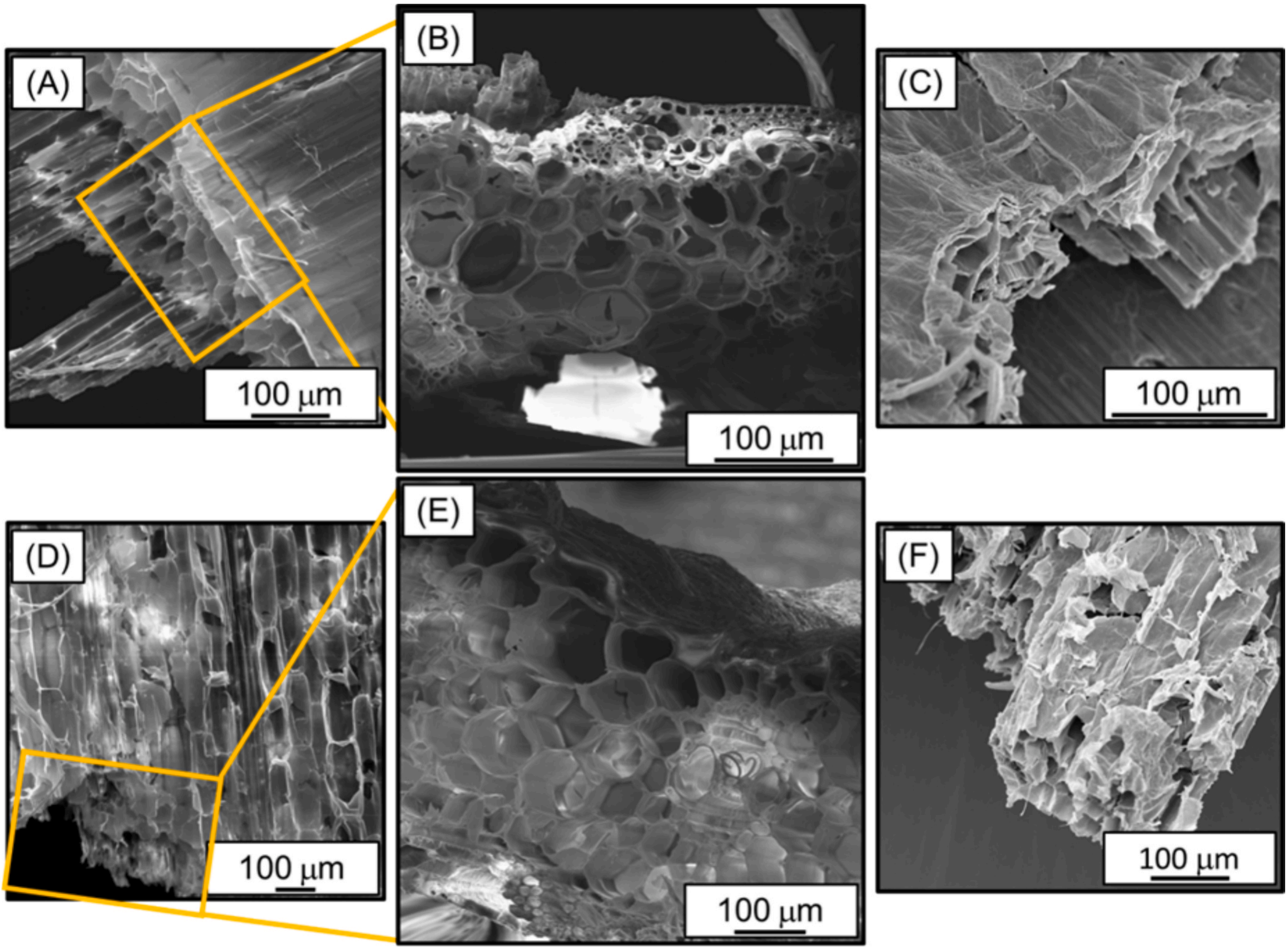

**Fig. 2.** Scanning electron microscopy images of; (A) leached barley straw 1–2 mm, (B) rotated leached barley straw 1–2 mm, (C) Barley straw 0.2 M NaOH sludge (30 min), (D) leached wheat straw 1–2 mm, (E) rotated leached wheat straw 1–2 mm and (F) Wheat straw 0.2 M NaOH (30 min) sludge.

show that the sludge feedstocks experience a single broad thermal event where they lose the majority of their mass (loss of volatile components), these figures are Fig. 3**b** and Fig. 3**d** for barley straw and wheat straw derived sludges, respectively. The first derivative weight loss for the barley straw sludge was found between 317.7 °C and 335.6 °C where the barley straw sludge feedstocks hydrolysed for the longer residence time (60 min) were all found to shift to slightly higher temperature. This was not echoed by the wheat straw sludge family which all appear to have a mass loss around the same temperature 323.4 °C and 329.8 °C, a + 6.4 °C variation compared to + 17.9 °C seen for barley straw sludge. The major differences for sludge-derived feedstocks are their direct comparison with their parent leached feedstocks. Fig. 3**b** and Fig. 3**d** present overlaid parent feedstock data in black dots, across both feedstocks, this appears as two distinct peaks 273.2 °C and 339.0 °C for leached barley straw compared with 274.5 °C and 337.7 °C for leached wheat straw. The initial peak found in the DTG curves has been previously characterized as the depolymerisation of hemicellulose and pectins [30,48]. This aligns strongly with the role of the NaOH in the hydrolysis reaction, sugar molecules have been removed from the feedstocks and pectins are heteropolysaccharides that have been removed from the lignin polymer backbone. However, the DTG figures (Fig. 3**b** and Fig. 3**d**) do not indicate if there is any observable effect of using higher concentrations of NaOH as the initial peak seen in the feedstock is effectively removed after 30 min in a 0.2 M NaOH solution, albeit **Table S1** shows a steady increase of sugar removal in line with rising NaOH concentrations. The thermal degradation profiles align with some of the recent studies on NaOH-pretreated biomass. Evans et al. observed similar shifts to higher decomposition temperatures (~320–340 °C) for sugarcane bagasse after NaOH pre-treatment, attributing this to lignin enrichment and reduced hemicellulose [49]. Likewise, the single broad mass-loss peak for sludges (Fig. 3**b** and Fig. 3**d**) matches observations by our previous work on leached pine wood, where ash removal minimized catalytic interference during devolatilization [33].

### *3.2. The gasification of biorefinery sludges*

As far, there has been little evidence, other than sugar removal to suggest that a longer hydrolysis residence time will benefit the feedstock as they look very similar in terms of their FTIR spectra (Fig. 1) and thermal degradation profiles (Fig. 3), their calorific values, C/H ratios, HHV and LHV are all similar for the 30 min and 60 min hydrolysis treatments. Fig. 4 presents the gas phase product distributions across the three NaOH concentrations, where Fig. 4**a** shows the producer gas after 30 min hydrolysis time on the feedstocks and Fig. 4**b** presents the product mix from the 60 min hydrolysed materials. Comparing Fig. 4**a** and Fig. 4**b**, with Table 2 for clarity, the data shows a strong trend that hydrogen production can be promoted by increasing the NaOH concentration above 0.2 M for 30 min reaction time. For the 0.4 M NaOH (Fig. 4**a**) the hydrogen yield reached 27.95 vol.%, this is 72.7 % higher than the hydrogen yield for 0.2 M NaOH. For direct comparison, the parent leached feedstock (no base pre-treatment) was gasified using the same operational conditions mentioned previously. Table 2 shows that

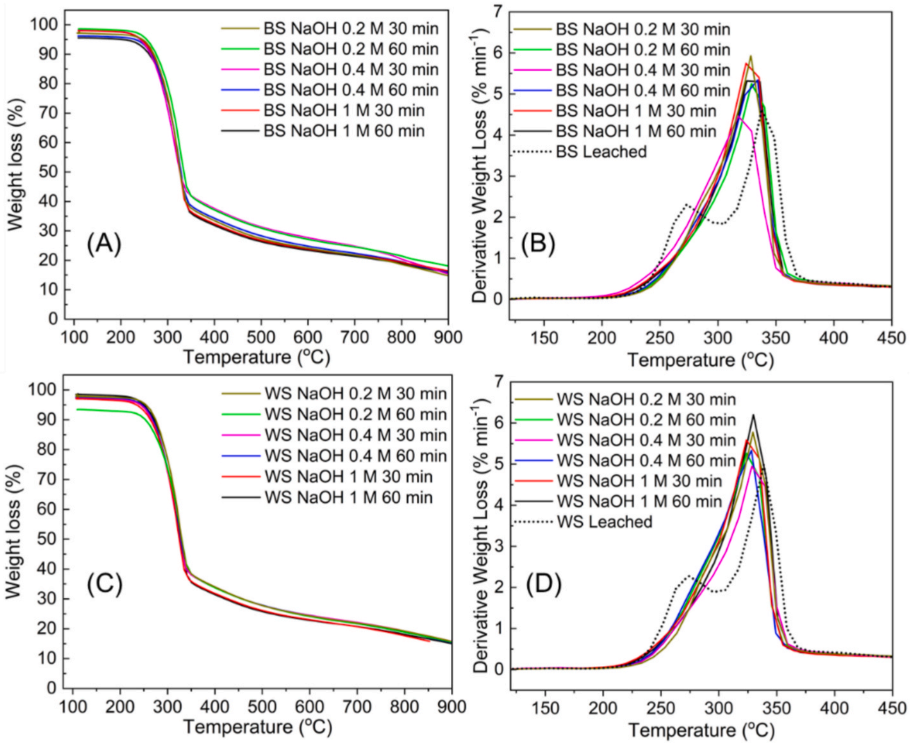

**Fig. 3.** Thermogravimetric weight loss and DTG curve for barley straw (BS) derived sludges, (A and B, respectively) and wheat straw (WS) derived sludges (C and D, respectively).

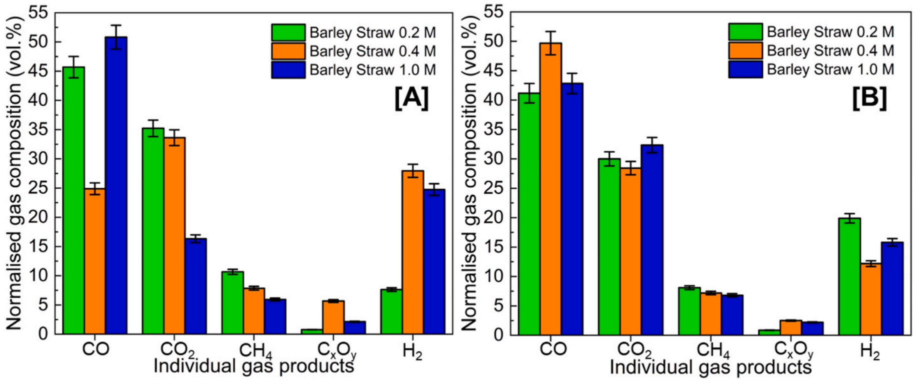

**Fig. 4.** Gasification reaction product mix data for barley straw sludges (A) after 30 min hydrolysis and (B) after 60 min hydrolysis.

**Table 2**
Gasification reaction gas phase product mix, averaged triplicate runs (vol.%) and overall reaction selectivity (wt.%).

| Feedstock | CO (vol.%) | $CO_2$ (vol.%) | $CH_4$ (vol.%) | $C_xH_y$ (vol.%) | $H_2$ (vol.%) | Solid (wt.%) | Liquid (wt.%) | Gas (wt.%) |
|---|---|---|---|---|---|---|---|---|
| BS Leached Feedstock | 44.15 | 39.26 | 10.43 | 2.02 | 4.15 | 17.84 | 32.33 | 49.83 |
| BS 0.2 M NaOH 30 min | 45.69 | 35.23 | 10.67 | 0.78 | 7.63 | 10.79 | 17.50 | 71.70 |
| BS 0.2 M NaOH 60 min | 41.17 | 30.00 | 8.09 | 0.85 | 19.89 | 7.66 | 17.03 | 75.31 |
| BS 0.4 M NaOH 30 min | 24.89 | 33.62 | 7.86 | 5.68 | 27.95 | 8.49 | 18.09 | 73.42 |
| BS 0.4 M NaOH 60 min | 49.69 | 28.44 | 7.19 | 2.50 | 12.19 | 10.73 | 8.86 | 80.41 |
| BS 1.0 M NaOH 30 min | 50.83 | 16.34 | 5.94 | 2.15 | 24.75 | 10.52 | 16.58 | 72.90 |
| BS 1.0 M NaOH 60 min | 42.83 | 32.35 | 6.80 | 2.21 | 15.81 | 12.01 | 14.17 | 73.82 |
| WS Leached Feedstock | 66.30 | 12.05 | 6.58 | 3.56 | 11.51 | 7.41 | 31.90 | 60.69 |
| WS 0.2 M NaOH 30 min | 32.86 | 51.64 | 7.75 | 2.11 | 5.63 | 37.60 | 18.87 | 43.53 |
| WS 0.2 M NaOH 60 min | 40.79 | 25.00 | 10.71 | 1.43 | 22.06 | 50.02 | 17.11 | 32.88 |
| WS 0.4 M NaOH 30 min | 40.60 | 28.68 | 9.95 | 1.57 | 19.20 | 10.80 | 17.08 | 72.12 |
| WS 0.4 M NaOH 60 min | 37.96 | 29.29 | 10.14 | 1.53 | 21.08 | 10.50 | 17.78 | 71.72 |
| WS 1.0 M NaOH 30 min | 41.44 | 26.82 | 8.33 | 1.29 | 22.12 | 11.59 | 16.70 | 71.71 |
| WS 1.0 M NaOH 60 min | 40.57 | 29.26 | 10.64 | 1.69 | 17.84 | 29.83 | 16.00 | 54.17 |

the parent barley straw feedstock only yielded 4.15 vol.% $H_2$, where the 0.4 M NaOH, 30 min sample enabled an 85.2 % increase in hydrogen yield. Furthermore, the base hydrolysis reaction (0.4 M NaOH, 30 min) generated 32.1 % more gas phase products than the virgin barley straw. In fact, by depolymerising the hemicellulose, weakening the interactions with the lignin backbone (Fig. 1**a** and Fig. 3**b**), all hydrolysed barley straw sludges generated more gas phase products than the leached feedstock alone, clearly demonstrating the benefit of combining hydrolysis with leaching for enhancing valuable gasification products. Additionally, the use of base as a pre-treatment has been found in the past to lower the crystallinity index (CrI) of cellulose itself. Clearly, **Table S2** shows that not all the cellulose was removed from the initial feedstock, across both the various NaOH concentrations and short residence times. Therefore, one can infer that the CrI will have decreased through the pre-treatment process, similarly to how our previous work demonstrated it could be achieved using water alone, this has been established previously for promoting the enzymatic conversion of cellulose through increased accessibility [33,50,51]. Another benefit shown in Fig. 4**a** is that the volume of $CO_2$ created has been substantially lowered in favour of the partially oxidized $CO_x$, CO, a marketable product for heating and chemical production through route such as the Fischer–Tropsch process when reacted with hydrogen over a catalytic package [52]. Due to a steady decrease in methane as base concentration increases, Fig. 4**a**, one may infer that there has been some methane reforming taking place (Eq. **(4)** which directly aligns with the increases in CO and $H_2$. This is echoed further in Fig. 4**b**, which shows the exact same trend, albeit subtly lower. In the interest of promoting hydrogen production as a sustainable low-carbon fuel source, Fig. 4**b** infers that a prolonged residence time is only beneficial for hydrogen production if a low NaOH concentration is used for barley straw. This is where 0.2 M NaOH, 60 min produced 19.89 vol.% $H_2$, this is 61.6 % higher than the 30 min hydrolysis counterpart. Moreover, the barley straw pretreated with 0.2 M NaOH, 60 min produced 79.1 % more hydrogen than leached barley straw alone. The 60 min residence time for 0.4 M NaOH, barley straw sludge was found to produce far more CO than its 30 min counterpart (49.9 %, Table 2). This selectivity swap could be due to the higher ash content in 0.4 M NaOH, 60 min barley straw sludge than the 30 min equivalent (Table 1), possibly in the form of Na cations that were not solubilised and catalysing the water–gas shift reaction [16], favouring CO whereas the 0.4 M NaOH, 30 min barley straw sludge possessed a higher moisture content, which could push the equilibrium towards $H_2$ production in place of carbonaceous molecules.

For the case of wheat straw derived sludges, Fig. 5**a** and Fig. 5**b** show the effect of hydrolysing the waste stream for 30 min and 60 min, respectively. In a very similar trend with barley straw sludges, a higher NaOH concentration generates a higher hydrogen yield, only when a shorter residence time is used. As explained previously in Fig. 4**b**, Fig. 5**b** shows that product selectivity favours a weaker NaOH concentration if following a 60 min residence time, producing more $CO_2$, $CH_4$ and $C_xH_y$ in favour of $H_2$ when using a sludge hydrolysed with 1.0 M NaOH.

Table 2 clearly shows that wheat straw sludges all produce more $H_2$ for a 60 min residence time, vs their 30 min counterparts (with the exception of the 1.0 M NaOH, which is slightly lower). Except for 0.2 M NaOH, 30 min, all wheat straw sludges, alike their barley straw comparators produce more $H_2$ than the leached parent feedstock, the deviation in the trend for the feedstock mentioned is proposed to be experimental variance in place of bucking the proposed $H_2$ trend, as suggested by a higher $CO_2$ concentration than all the other sludge feedstocks. Fig. 4 and Fig. 5 do show that base pre-treatment can be optimized where 0.4 M NaOH is clearly beneficial for promoting hydrogen production across both feedstocks.

For barley straw, the optimum reaction conditions for base hydrolysis were found to be 0.4 M NaOH for 30 min to achieve the maximum hydrogen yield. Wheat straw sludges did see a marginal increase in $H_2$ product concentration when the 1.0 M NaOH was used for 30 min. Between the two sludges, if the 0.4 M NaOH 30 min pre-treatment regime were to be used, there would be 31.3 % less hydrogen produced if using wheat straw instead of barley straw, indicating that barley straw is more favourable for this process but wheat straw is still effective, albeit produces 61 % more CO than barley straw. An interesting caveat for the 60 min wheat straw sludges (Fig. 5**b**), there is an increase in methane yield, across all base concentrations, this is only seen for this feedstock showing a higher affinity towards $CH_4$ in place of $C_xH_y$ residues that are observed for barley straw derived sludges.

The $H_2$ yields achieved in this work (27.95 vol.% for barley straw, 22.12 vol.% for wheat straw) are competitive with some of the previous works in biomass gasification. Gong et al. reported 99.93 vol.% $H_2$ purity using a complex cascade process (alkaline thermal treatment + catalytic steam reforming + alkali absorption), which requires a Ni catalyst, high NaOH loads, and multi-stage reactors [37]. In contrast, our single-step gasification offers comparable yields without the need for catalysts, steam, or energy-intensive purification steps. These results represent a significant improvement over conventional biomass gasification systems: Duman and Yanik achieved only 15–20 vol.% $H_2$ from steam gasification of wheat straw [38], while Sharma et al., reported 18–20 vol.% $H_2$ from catalytic gasification of Lantana camara biomass [39]. The effectiveness of our NaOH-sludge pre-treatment is further highlighted by matching work by Meng et al., who achieved 20–28 vol.% $H_2$ from steam gasification of Agrol and willow [40] which surpassed more recent work by Yim et al., who reported a maximum hydrogen yield of 18.31 vol.% through the catalytic gasification of woody sawdust [41], whereas our system attained similar, if not higher yields in some cases without additional steam and or catalytic intervention. This work shows that physically, the outer structure of the feedstocks has changed demonstrating disorder (Fig. 2), chemically the sugar components have been removed or depolymerised (**Table S2** and Fig. 3, respectively), which has led to a change in products formed (Table 2). Assuming that less energy is physically needed to break the bonding post hydrolysis

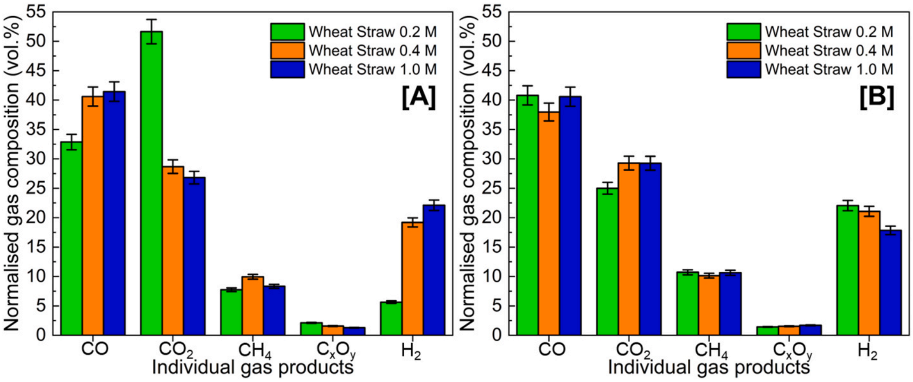

**Fig. 5.** Gasification reaction product mix data for wheat straw sludges (A) after 30 min hydrolysis and (B) after 60 min hydrolysis.

(reduction in cellulose crystallinity index), the concentration of gas phase products has radically increased, especially towards hydrogen.

## 4. Conclusions

To prevent further release of unregulated carbon dioxide into the atmosphere, we need to make a step change in the way we globally produce energy, one such change is the use of sustainably generated hydrogen. With rapid research and development into the scale-up of hydrogen production, it is still driven by carbon-emitting processes. This work highlights a potential direction by utilizing a waste stream generated downstream of a lignocellulosic waste processing regime where sugar is extracted for further value-adding. The remaining sludge can be rapidly reformed and repurposed into a sustainable hydrogen feedstock that can be accessed via conventional gasification. By optimizing the waste pre-treatment process (independent of the feedstock used), the hydrogen yield can be enhanced. It has been shown that hydrogen production can be improved by 85.2 % for a hydrolysis sludge, when comparing to the parent feedstocks, prior to pre-treatment. The mentioned sludges are residual high moisture waste streams after hexose and pyranose sugar extraction. It is shown that barley and wheat straws can be valorized in a similar way where hydrogen yields were found to be ~50 % higher for hydrolysed sludges than the parent wheat straw feedstock, prior to base pre-treatment.

## CRediT authorship contribution statement

**Martin J. Taylor:** Writing – review & editing, Writing – original draft, Supervision, Project administration, Methodology, Funding acquisition, Formal analysis, Conceptualization. **Karl Hornsby:** Writing – original draft, Methodology, Formal analysis, Data curation. **Kin Wai Cheah:** Writing – review & editing, Writing – original draft, Investigation, Formal analysis. **Adrian Chun Minh Loy:** Writing – review & editing, Visualization, Validation, Formal analysis. **Peter Hurst:** Writing – review & editing, Methodology, Formal analysis, Conceptualization. **Mark Gronnow:** Writing – review & editing, Visualization, Investigation. **Katie Chong:** Writing – review & editing, Formal analysis. **Patrick Kelly:** Writing – review & editing, Investigation. **Simon Walker:** Writing – review & editing, Visualization, Investigation, Conceptualization. **Vasiliki Skoulou:** Writing – review & editing, Visualization, Methodology, Investigation, Data curation.

## Declaration of competing interest

The authors declare that they have no known competing financial interests or personal relationships that could have appeared to influence the work reported in this paper.

## Acknowledgements

The authors would like to thank the Department for Energy Security & Net Zero (DESNZ, UK Government) for funding the Bluegen project via the Hydrogen BECCS Innovation Programme: Phase 1. We would also like to thank Mr Philip Lawless for preparing initial feedstocks at scale and Dr Jason Dale for fruitful discussions. The authors would also like to thank Mr Timothy Dunstan for the acquisition of HRSEM images.

## Appendix A. Supplementary data

Supplementary data to this article can be found online at https://doi.org/10.1016/j.ecmx.2025.101135.

## Data availability

Data will be made available on request.

## References

[1] Cai J, He Y, Yu X, Banks SW, Yang Y, Zhang X, et al. Review of physicochemical properties and analytical characterization of lignocellulosic biomass. Renew. Sustain. Energy Rev. 2017;76:309–22.

[2] Isikgor FH, Becer CR. Lignocellulosic biomass: a sustainable platform for the production of bio-based chemicals and polymers. Polym. Chem. 2015;6:4497–559.

[3] Freitas EN, Salgado JCS, Alnoch RC, Contato AG, Habermann E, Michelin M, et al. Challenges of Biomass utilization for Bioenergy in a climate Change Scenario. Biology (basel) 2021;10.

[4] Taylor M, Alabdrabalameer H, Skoulou V. Choosing Physical, Physicochemical and Chemical Methods of Pre-Treating Lignocellulosic Wastes to Repurpose into Solid Fuels. Sustainability 2019;11.

[5] Farias CBB, Barreiros RCS, da Silva MF, Casazza AA, Converti A, Sarubbo LA. Use of Hydrogen as fuel: a Trend of the 21st Century. Energies 2022;15.

[6] Wappler M, Unguder D, Lu X, Ohlmeyer H, Teschke H, Lueke W. Building the green hydrogen market – current state and outlook on green hydrogen demand and electrolyzer manufacturing. Int. J. Hydrogen Energy 2022;47:33551–70.

[7] Taylor MJ. Bluegen: Utilisation of Biorefinery Residues for Blue Hydrogen Production - Closure Report, Hydrogen BECCS Innovation Programme: phase 1. United Kingdom: DESNZ; 2022.

[8] Rasul MG, Hazrat MA, Sattar MA, Jahirul MI, Shearer MJ. The future of hydrogen: challenges on production, storage and applications. Energ. Conver. Manage. 2022;272.

[9] Ishaq H, Dincer I, Crawford C. A review on hydrogen production and utilization: challenges and opportunities. Int. J. Hydrogen Energy 2022;47:26238–64.

[10] Singh Aulakh DJ, Boulama KG, Pharoah JG. On the reduction of electric energy consumption in electrolysis: a thermodynamic study. Int. J. Hydrogen Energy 2021;46:17084–96.

[11] Andriani D, Bicer Y. A Review of Hydrogen Production from Onboard Ammonia Decomposition: Maritime applications of Concentrated Solar Energy and Boil-off Gas Recovery. Fuel 2023;352:128900.

[12] Fincke JR, Anderson RP, Hyde TA, Detering BA. Plasma Pyrolysis of methane to Hydrogen and Carbon Black. Ind. Eng. Chem. Res. 2002;41:1425–35.

[13] Weber CL, Clavin C. Life cycle carbon footprint of shale gas: review of evidence and implications. Environ. Sci. Technol. 2012;46:5688–95.

[14] Taylor MJ, Michopoulos AK, Zabaniotou AA, Skoulou V. Probing Synergies between Lignin-Rich and Cellulose Compounds for Gasification. Energies 2020;13.

[15] Molino A, Chianese S, Musmarra D. Biomass gasification technology: the state of the art overview. Journal of Energy Chemistry 2016;25:10–25.

[16] Arnold RA, Hill JM. Catalysts for gasification: a review. Sustainable Energy Fuels 2019;3:656–72.

[17] Song C, Zhang C, Zhang S, Lin H, Kim Y, Ramakrishnan M, et al. Thermochemical liquefaction of agricultural and forestry wastes into biofuels and chemicals from circular economy perspectives. Sci. Total Environ. 2020;749:141972.

[18] Skoulou V, Zabaniotou A. Fe catalysis for lignocellulosic biomass conversion to fuels and materials via thermochemical processes. Catal. Today 2012;196:56–66.

[19] Skoulou V, Zabaniotou A, Stavropoulos G, Sakelaropoulos G. Syngas production from olive tree cuttings and olive kernels in a downdraft fixed-bed gasifier. Int. J. Hydrogen Energy 2008;33:1185–94.

[20] Priyanka IE, Wood A, Al-Gailani BW, Kolosz KW, Cheah D, Vashisht SK, et al. Taylor, cleaning up Metal Contamination after decades of Energy Production and Manufacturing: reviewing the Value in use of Biochars for a Sustainable Future. Sustainability 2024;16.

[21] Baurhoo B, Ruiz-Feria CA, Zhao X. Purified lignin: Nutritional and health impacts on farm animals—A review. Anim. Feed Sci. Technol. 2008;144:175–84.

[22] Siahkamari M, Emmanuel S, Hodge DB, Nejad M. Lignin-Glyoxal: a fully Biobased Formaldehyde-Free Wood Adhesive for Interior Engineered Wood Products. ACS Sustain. Chem. Eng. 2022;10:3430–41.

[23] Ekielski A, Mishra PK. Lignin for Bioeconomy: the present and Future Role of Technical Lignin. Int. J. Mol. Sci. 2020;22.

[24] Sethupathy S, Murillo Morales G, Gao L, Wang H, Yang B, Jiang J, et al. Lignin valorization: Status, challenges and opportunities. Bioresour. Technol. 2022;347:126696.

[25] Sharma A, Kaur P, Singh G, Arya SK. Economical concerns of lignin in the energy sector. Cleaner Eng. Technol. 2021;4.

[26] Cao L, Yu IKM, Xiong X, Tsang DCW, Zhang S, Clark JH, et al. Biorenewable hydrogen production through biomass gasification: a review and future prospects. Environ. Res. 2020;186:109547.

[27] Kumar A, Singh Negi Y, Choudhary V, Kant Bhardwaj N. Characterization of Cellulose Nanocrystals Produced by Acid-Hydrolysis from Sugarcane Bagasse as Agro-Waste. Journal of Materials Physics and Chemistry 2020;2:1–8.

[28] Mendu V, Harman-Ware AE, Crocker M, Jae J, Stork J, Morton 3rd S, et al. Identification and thermochemical analysis of high-lignin feedstocks for biofuel and biochemical production. Biotechnol. Biofuels 2011;4:43.

[29] Alvira P, Tomas-Pejo E, Ballesteros M, Negro MJ. Pre-treatment technologies for an efficient bioethanol production process based on enzymatic hydrolysis: a review. Bioresour. Technol. 2010;101:4851–61.

[30] Taylor MJ, Hornsby K, Cheah KW, Hurst P, Walker S, Skoulou V. Repurposing lignin rich biorefinery waste streams into the next generation of sustainable solid fuels. Sustainable Chemistry for the Environment 2024;7.

[31] Alabdrabalameer HA, Taylor MJ, Kauppinen J, Soini T, Pikkarainen T, Skoulou V. Big problem, little answer: overcoming bed agglomeration and reactor slagging during the gasification of barley straw under continuous operation. Sustainable Energy Fuels 2020;4:3764–72.

[32] Alabdrabalameer HA, Taylor MJ, Kauppinen J, Soini T, Pikkarainen T, Skoulou V. Big problem, little answer: overcoming bed agglomeration and reactor slagging during the gasification of barley straw under continuous operation. Sustainable Energy Fuels 2020.

[33] Taylor MJ, Alabdrabalameer HA, Michopoulos AK, Volpe R, Skoulou V. Augmented Leaching Pre-treatments for Forest Wood Waste and their effect on Ash Composition and the Lignocellulosic Network. ACS Sustain. Chem. Eng. 2020;8:5674–82.

[34] Vamvuka D, Zografos D, Alevizos G. Control methods for mitigating biomass ash-related problems in fluidized beds. Bioresour. Technol. 2008;99:3534–44.

[35] Lacey JA, Aston JE, Thompson VS. Wear Properties of Ash Minerals in Biomass. Front. Energy Res. 2018;6.

[36] Niu M, Fu Y, Liu S. Mineralogical Characterization of Gasification Ash with Different Particle Sizes from Lurgi Gasifier in the Coal-to-Synthetic Natural Gas Plant. ACS Omega 2022;7:8526–35.

[37] Gong X, Lu H, Liu G, Wu K, Liang B. High-purity H2 production from biomass through cascade processes based on alkaline thermal treatment. Int. J. Hydrogen Energy 2025;98:148–58.

[38] Duman G, Yanik J. Two-step steam pyrolysis of biomass for hydrogen production. Int. J. Hydrogen Energy 2017;42:17000–8.

[39] Sharma PK, Sharma AK, Pulla RH, Sahoo PK. Performance analysis of a medium-scale downdraft gasifier using Lantana camera biomass as feeding material. Energy Sources Part A 2020;46:15087–101.

[40] Meng X, de Jong W, Fu N, Verkooijen AHM. Biomass gasification in a 100 kWth steam-oxygen blown circulating fluidized bed gasifier: Effects of operational conditions on product gas distribution and tar formation. Biomass Bioenergy 2011;35:2910–24.

[41] Yim H, Valizadeh S, Pyo S, Jang S-H, Ko CH, Khan MA, et al. Hydrogen generation from gasification of woody biomass upon acid mine drainage sludge as a novel catalyst under an air medium. Fuel 2023;338.

[42] Priyanka D, Vashisht MJ, Taylor SK. Mehta, evaluating the pre-treatment protocol required to produce an effective carbonized waste adsorbent for organic pollution control. Front. Environ. Sci. 2023;11.

[43] Liang J, Lin Y, Li T, Mo F. Microbial consortium OEM1 cultivation for higher lignocellulose degradation and chlorophenol removal. RSC Adv. 2017;7:39011–7.

[44] Bhagia S, Ďurkovič J, Lagaňa R, Kardošová M, Kačík F, Cernescu A, et al. Nanoscale FTIR and Mechanical Mapping of Plant Cell Walls for Understanding Biomass Deconstruction. ACS Sustain. Chem. Eng. 2022;10:3016–26.

[45] J. Zhuang, M. Li, Y. Pu, A. Ragauskas, C. Yoo, Observation of Potential Contaminants in Processed Biomass Using Fourier Transform Infrared Spectroscopy, Applied Sciences, 10 (2020).

[46] Parihar A, Vongsvivut J, Bhattacharya S. Synchrotron-based Infra-Red Spectroscopic Insights on Thermo-Catalytic Conversion of Cellulosic Feedstock to Levoglucosenone and Furans. ACS Omega 2019;4:8747–57.

[47] Cotrim AR, Ferraz A, Gonçalves AR, Silva FT, Bruns RE. Identifying the origin of lignins and monitoring their structural changes by means of FTIR-PCA and -SIMCA. Bioresour. Technol. 1999;68:29–34.

[48] Castro RI, Morales-Quintana L. Study of the cell wall components produced during different ripening stages through thermogravimetric analysis. Cellul. 2019;26:3009–20.

[49] Evans SK, Wesley ON, Nathan O, Moloto MJ. Chemically purified cellulose and its nanocrystals from sugarcane baggase: isolation and characterization. Heliyon 2019;5:e02635.

[50] Park S, Baker JO, H.M. E, P.A. Parilla, D. Johnson,. Cellulose crystallinity index: mesurement techniques and their impact on interpreting cellulase performance. Biotechnol. Biofuels 2010;3.

[51] Xu H, Che X, Ding Y, Kong Y, Li B, Tian W. Effect of crystallinity on pre-treatment and enzymatic hydrolysis of lignocellulosic biomass based on multivariate analysis. Bioresour. Technol. 2019;279:271–80.

[52] Lim JY, Loy ACM, Alhazmi H, Fui BCL, Cheah KW, Taylor MJ, et al. Machine learning–assisted CO2 utilization in the catalytic dry reforming of hydrocarbons: Reaction pathways and multicriteria optimization analyses. Int. J. Energy Res. 2021;46:6277–91.